International Journal of Electrical, Electronic and Communication Sciences
ISSN: 2517-9438
Vol:9, No:8, 2015

Effect of Atmospheric Turbulence on Hybrid FSO/RF Link Availability under Qatar Harsh Climate

Abir Touati, Syed Jawad Hussain, Farid Touati, Ammar Bouallegue

***Abstract*—**Although there has been a growing interest in the hybrid free-space optical link and radio frequency FSO/RF communication system, the current literature is limited to results obtained in moderate or cold environment. In this paper, using a soft switching approach, we investigate the effect of weather inhomogeneities on the strength of turbulence hence the channel refractive index under Qatar harsh environment and their influence on the hybrid FSO/RF availability. In this approach, either FSO/RF or simultaneous or none of them can be active. Based on soft switching approach and a finite state Markov Chain (FSMC) process, we model the channel fading for the two links and derive a mathematical expression for the outage probability of the hybrid system. Then, we evaluate the behavior of the hybrid FSO/RF under hazy and harsh weather. Results show that the FSO/RF soft switching renders the system outage probability less than that of each link individually. A soft switching algorithm is being implemented on FPGAs using Raptor code interfaced to the two terminals of a 1Gbps/100 Mbps FSO/RF hybrid system, the first being implemented in the region. Experimental results are compared to the above simulation results.

***Keywords*—**Atmospheric turbulence, haze, soft switching, Raptor codes, refractive index.

I. Introduction

HYBRID free-space optical/radio frequency (FSO/RF) links have taken a big interest due to their advantages. FSO/RF is an effective and competitive solution for high-speed applications and wireless communications [1]. It combines the benefits of two complementary subsystems; the high data rate ensured by the FSO link which can exceed 1Gb/s and a reliable RF link which serves a backup. The biggest challenge for an FSO link is the weather condition, (e.g., fog, haze...). Harsh climate may cause the degradation of optical signal whereas the RF link is not sensitive to the weather but suffers only from the rain scatter [2], [3]. Thus, using the two links in a system allows overcoming these unique channel impairments and ensures a high data rate. There are two configurations of hybrid FSO/RF links. In [4], the authors have presented the first configuration called hard switching. In this approach, the transmitter and receiver are coordinated to select the appropriate channel for data transmission. Thus, only one channel is active at any time. FSO link will be selected only if the channel conditions are favorable to provide a reliable transmission. Otherwise the RF link will be selected. The disadvantage of this hard switching approach is that the RF link can be selected for a large period, and hence the channel capacity of FSO link is wasted. In, order to overcome this issue, a new configuration of hybrid FSO/RF, called soft switching, is involved. In this setting, the two links are working simultaneously by using the channel coding. In fact, several studies are attempted to evaluate the influence of channel coding on hybrid FSO/RF. In [5], the authors have investigated the performance of Turbo codes for FSO/RF systems. They have found that these codes enable the hybrid to maintain a certain level of error probability. In [6], Zhang and al. have studied the soft switching by using the Raptor codes. Based on experimental results, they have found that the encoded system can provide significantly higher throughputs particularly in adverse weather condition.

In order to evaluate the performance of hybrid system under a dry and harsh climate, we designed and implemented a practical soft switching configuration. The hybrid FSO/RF has been installed in Qatar University (QU), Doha, Qatar. The two sub-systems have been installed at two different buildings separated by a distance of 600 m. FSO system uses an optical transceiver at 1550 nm wavelength. The hybrid has a capacity of 1 Gb/s, and 100 Mbps for FSO and RF, respectively.

The remainder of this paper is organized as follows. Section II details the different causes of atmospheric attenuation for FSO link. The channels modeling of FSO and RF links are presented in Section III. In Section IV, based on Markov chain process, the outage probability expression of the hybrid systems is derived. Then, a background of Raptor code is presented in Section V. After that, the design and the implementation model of channel coding used in our work is described in Section VI. In Section VII, the performances of FSO/RF channels under different strength of turbulence and under hazy weather related to Qatar climate are investigate. And a comparison between the behavior of FSO link with un-coded data and the hybrid FSO/RF with encoded data is conducted.

II. Atmospheric Turbulence

Atmospheric attenuation is defined as the phenomenon whereby the transmitted optical signal is lost when it is emitted through the atmosphere. Indeed, the optical waves are very sensitive to the atmospheric turbulence which can cause attenuation and signal degradation of optical wave in several

Abir Touati is with the Electrical Engineering Department, Qatar University and PhD student at SYSCOM, National School of Engineering, Tunisia (e-mail: abirtouati@ qu.edu.qa)

Syed Jawad Hussain is with the Electrical Engineering Department, Qatar, (e-mail: s.jawad@qu.edu.qa).

Farid Touati was with Nagoya Institute of Technology, Japan and Tuskegee University, Alabama, USA. He is now with the Electrical Engineering Department, Qatar University, Qatar, (e-mail: touatif@qu.edu.qa).

A. Bouallegue is with SYSCOM, National Engineering School of Tunis, University Tunis El Manar, (e-mail: ammarbouallegue.syscom@gmail).

ways including absorption, scattering, and scintillation.

A. Absorption

This phenomenon results from the interaction between the incidents photons and the atoms/molecules in the atmosphere which leads to the disappearing of the incident photon [7]. In order to reduce the absorption effect and even to neglect it, all the FSO systems use a wavelength that falls into the atmospheric transmission windows [8]. For this reason, in our study the effect of absorption is neglected.

B. Scintillation

Scintillation called also atmospheric turbulence is caused by air turbulence and leads to the appearance of fluctuations in both the intensity and phase of the received light signal. And hence, causes the impairing of link performance as shown in Fig. 1.

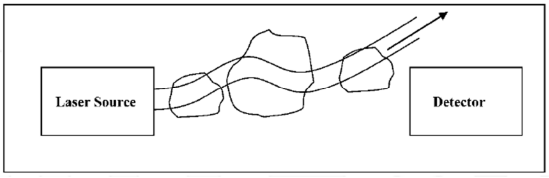

Fig. 1 Scintillation or fluctuations in beam intensity at the receiver

Atmospheric turbulence depends strongly on weather conditions which cause variations on the refractive index [8]. The expression of scintillation index is given by [9]:

$$\sigma_I = \exp\left[\frac{0.49\beta^2}{\left(1+0.18d^2+0.56\beta^{\frac{12}{5}}\right)^{\frac{7}{6}}}+\frac{0.51\beta^2\left(1+0.69\beta^{\frac{12}{5}}\right)}{\left(1+0.9d^2+0.62d^2\beta^{\frac{12}{5}}\right)^{\frac{7}{6}}}\right]-1, \quad (1)$$

where d is related to the wavelength λ and the link distance L between transmitter and receiver as:

$$d = \sqrt{\frac{2\pi}{4\lambda L}}D. \quad (2)$$

The second parameter β is formally the same as the Rytov relative variance of optical intensity for spherical waves [9], β is a function of refractive index C_n^2, the wave number and the link distance L, respectively. C_n^2 is formulated as:

$$\beta^2 = 0.5C_n^2 k^{\frac{7}{6}} L^{\frac{11}{6}}. \quad (3)$$

C. Refractive Index

The refractive index structure parameter C_n^2 is the most significant parameter that determines the turbulence strength. It depends on various factors. In [8], Majumdar has investigated the dependence of refractive index on the geographical location and altitude. More the altitude increases more the refractive index decreases. For this reason the larger values of C_n^2 is reached at sea level. In [9], the authors have found mathematical expressions of the refractive index as a function of weather parameters (temperature, wind and humidity). They have showed the effect of the day time and the season on the variation of C_n^2. However, many models have been formulated to describe the refractive index profile C_n^2 and among those, one of the widely used models is the Hufnagel-Valley which is given by:

$$C_n^2 = A\exp\left(-\frac{h}{100}\right) + 0.005941 \cdot (10^{-5}h)^{10}.\left(\frac{V}{27}\right)^2 \cdot \exp\left(-\frac{h}{1000}\right) + 2.7\cdot 10^{-16}\exp\left(-\frac{h}{1500}\right), \quad (4)$$

where A is the refractive index structure parameter at ground level, equal to $1.7\ 10^{-14}m^{-2/3}$, V is the wind speed in m/s, and h is the altitude in meters. Moreover, as indicated above, the turbulence strength is dependent on weather conditions. In fact, according to [10], the expression of C_n^2 can be expressed as:

$$C_n^2(h) = C_n^2(h) + C_n^2(T, V, H, TCSA, SF), \quad (5)$$

where:

$$C_n^2(T,V,H,TCSA,SF) = 5.9\ 10^{-15}Wth + 1.6\ 10^{-15}T - 3.7\ 10^{-15}H - 3.7\ 10^{-15}V + 2.8\ 10^{-14}SF - 1.8\ 10^{-14}TCSA - 3.9\ 10^{-13} \quad (6)$$

Here, Wth is a temporal hour weight, T is the temperature in Kelvin, H is the relative humidity (%), SF is the solar flux in units of kW/m^2, and $TCSA$ is the total cross sectional area of the aerosol particles given by [10]:

$$TCSA = 3.7\ 10^{-3} + 9.96\ 10^{-4}H - 2.75\ 10^{-5}H^2 - 1.37\ 10^{-5}SF^4 \quad (7)$$

The C_n^2 was compiled for a typical Summer day in Doha using weather parameters. The results are shown in Fig. 2.

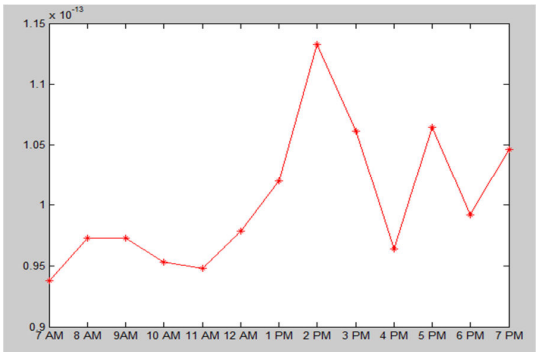

Fig. 2 The measurements of C_n^2 in a typical day of July in Doha (July 7)

As shown in Fig. 2, the C_n^2 is considered high in the order of 10^{-13}. This is due to the high temperature measured in Doha in the Summer season. In July 7, the temperature reached the 42 C between 12 AM and 3 PM. Moreover, the wind speed is considered high (from 23 to 32 *km/h*). In fact, the high level of temperature leads to heating up some air cells or air pockets and this causes variations of the refractive index which in turn causes an increase in the strength of turbulence.

D.Haze Attenuation

In Qatar, the weather is very dry in summer where the temperature can easily exceed the 45 C while in winter there is a very low level of precipitation. In autumn, the humidity reaches high levels and exceeds the 80%. The biggest challenge of FSO transmission in Qatar is the haze which is caused by many sources: dust, smoke and any particles emitted into the atmosphere caused the reduction of the visibility. Haze particles have the same size and sometimes a size greater than the wavelength of FSO sub system. For this reason, haze effect is classified under Mie scattering [7]. Scattering coefficient is given by Kim model. According to this model, the scattering coefficient depends on q: the scattering particles size distribution. Moreover, this parameter is inversely proportional to the atmospheric visibility *V*. Thus, low visibility means that the size and concentration of haze particles are high when compared on their state in the average and high visibility. Therefore, scattering and attenuation appear to be more when the visibility is low. In Qatar, the range of low visibility extends from 1 to 6 *km* and the range of average visibility extends from 6 to 10 *km*. The scattering coefficient is given by [9]:

$$\alpha = \frac{3.91}{V}\left(\frac{\lambda}{550}\right)^{-q}, \tag{8}$$

where the visibility is in kilometers, λ is the wavelength measured in nanometers and q is given as [2]:

$$q = \begin{cases} 1.3 & if\ V > 6\ km \\ 0.585 V^{\frac{1}{3}} & if\ V < 6\ km. \end{cases} \tag{9}$$

The atmospheric attenuation based on scattering coefficient can be calculated as:

$$\alpha_{haze} = 10 \log_{10} \exp\left[\left(\frac{\lambda}{550}\right)^{-q} L\right]. \tag{10}$$

III. Systems Modeling

A. FSO Channel

In free space optical communications, the received optical signal $r_1(t)$ has the following expression: $r_1(t) = e_1(t)\, h_{FSO}(t) + n_1(t)$, where $e_1(t)$ is the transmitted signal, $n_1(t)$ is the additive Gaussian noise and h_{FSO} is the FSO channel fading coefficient caused by the atmospheric turbulence. For such FSO channel, the instantaneous SNR can be defined as:

$$\gamma_{FSO}(t) = \overline{\gamma_{FSO}}\ h_{FSO}^2(t), \tag{11}$$

where $\overline{\gamma_{FSO}}$ is the average SNR defined by [11]:

$$\overline{\gamma_{FSO}} = \frac{h_{l1}^2\ R^2\ P_t^2}{\sigma_{n1}^2}, \tag{12}$$

R, P_t and ${\sigma_{n1}}^2$ are the FSO responsivity, average transmitted power and noise variance, respectively. h_{l1} is the path loss of FSO link which is given by [12]: $h_{l1} = [erf(\sqrt{A}/\theta L)]^2 \exp(-\alpha_1 L)$, *erf* is the error function, $A = \pi D^2$ is the area of receiver aperture, D is the receiver diameter in m, θ is the beam divergence, L is the link range in *km* and α_1 is the weather extinction given by (8). Taking into account that the fading of FSO channel has a coherent time slow compared to the typical symbol rates of FSO system [11]; $h_{FSO}(t)$ and $\gamma_{FSO}(t)$ can be assumed constant for a large number of transmitted data. Consequently, the FSO link outage will occurs when the received SNR falls below some threshold referred by γ_{thFSO}. The fading channel is modeled as a log normal distribution which has the probability distribution function (PDF) given by:

$$f(h_{FSO}) = \frac{1}{\sqrt{8\pi}\,\sigma_I\, h_{FSO}} \exp\left[\frac{\left(\ln(h_{FSO}) + {\sigma_I}^2\right)^2}{2\,{\sigma_I}^2}\right]. \tag{13}$$

Using (13) and [12], the PDF of $\gamma_{FSO} > 0$ can be written as:

$$f(\gamma_{FSO}) = \frac{1}{\sqrt{8\pi}\,\sigma_I \gamma_{FSO}} \exp\left[\frac{\left(\ln\sqrt{\frac{\gamma_{FSO}}{\overline{\gamma_{FSO}}}} + \frac{\sigma_I^2}{2}\right)^2}{2\sigma_I^2}\right]. \tag{14}$$

B. RF Channel

The RF used a line of sight (FOS) link and *M-ary* quadrature modulation *16-QAM*. The received signal can be written as: $r_2(t) = e_2(t) h_{RF}(t) + n_2(t)$; where $h_{RF}(t)$ is the RF channel coefficient, $e_2(t)$ is the QAM symbol and $n_2(t)$ is the noise term assumed to be complex zero-mean white Gaussian with variance of ${\sigma^2}_{n2}$. The instantaneous SNR of RF link is given by:

$$\gamma_{RF}(t) = \overline{\gamma_{RF}}\ h_{RF}^2(t), \tag{15}$$

where $\overline{\gamma_{RF}}$ is the RF average SNR defined by:

$$\overline{\gamma_{RF}} = \frac{h_{l2}\ P_t\ \log_2(M)}{\sigma_{n2}^2}, \tag{16}$$

h_{l2} is the path loss of RF link given by [12]. RF link is assumed to be available while the instanntaneous SNR is greater than some threshold termed γ_{thRF} (outage occurs while $\gamma_{RF} < \gamma_{thRF}$). The RF fading can be modulated by Rician distribution [12]. Thus, the PDF of $\gamma_{RF} > 0$ is given by:

$$f(\gamma_{RF}) = \frac{K+1}{\gamma_{RF}} \exp\left[-(k+1)\frac{\gamma_{RF}}{\gamma_{RF}} - K\right] \cdot I_0 \cdot \left[2\sqrt{K(K+1)\frac{\gamma_{RF}}{\gamma_{RF}}}\right], \quad (17)$$

where K is the Rician factor and I_0 is the zeroth-order modified Bessel function of the first kind.

IV. Finite State Markov Chain Model for Hybrid FSO/RF Systems

FSMC is used to derive mathematical expressions of hybrid outage probability which is a critical information in free space communication. Outage probability is defined as the probability that the instantaneous SNR falls below a certain threshold. In the soft switching approach, either FSO/RF channels or simultaneous or none of them can be active. Thus, our system model can be defined as a four-state Markov chain at any time n, $X_n \in \{S_0, S_1, S_2, S_3\}$, where:

S_0 : The two links are available.
S_1 : Only the FSO link is available.
S_2 : Only RF link is available.
S_3 : The two links are in outage

Markov model is characterized by the stationary state probability which is defined as the probability of being in the state k at any time n which is referred by:

$$\Pi(S_k) = Pr(X_n = S_k); k \in \{0,1,2,3\}.$$

Links outage depends on the thresholds γ_{thFSO} and/or γ_{thRF} pre-defined above. Thus, the stationary probabilities of the hybrid FSO/RF are given as:

$$\Pi(S_0) = \Pr(\gamma_{FSO} > \gamma_{thFSO}, \quad \gamma_{RF} > \gamma_{thRF}).$$
$$\Pi(S_1) = \Pr(\gamma_{FSO} > \gamma_{thFSO}, \quad \gamma_{RF} < \gamma_{thRF}).$$
$$\Pi(S_2) = \Pr(\gamma_{FSO} < \gamma_{thFSO}, \quad \gamma_{RF} > \gamma_{thRF}).$$
$$\Pi(S_3) = \Pr(\gamma_{FSO} < \gamma_{thFSO}, \quad \gamma_{RF} < \gamma_{thRF}).$$

Note that $\Pi(S_1), \Pi(S_2)$ and $\Pi(S_3)$ present: $P_{out}(RF)$, $P_{out}(FSO)$ and $P_{out}(hyb)$ which correspond respectively, to RF, FSO and hybrid outages. Taking into account that the γ_{FSO} and γ_{RF} are statistically independent, the outage probabilities are given by [12]:

$$P_{out}(RF) = (1 - F(\gamma_{thFSO}))\, F(\gamma_{thRF}).$$
$$P_{out}(FSO) = (1 - F(\gamma_{thRF}))\, F(\gamma_{thFSO}).$$
$$P_{out}(hyb) = F(\gamma_{thFSO})\ F(\gamma_{thRF}).$$

where $F(\gamma_{thFSO})$ and $F(\gamma_{thRF})$ are the cumulative distribution function of γ_{FSO} and γ_{RF} for γ_{thFSO} and γ_{thRF} respectively, and given as:

$$F(\gamma_{thFSO}) = Q\left(\frac{\ln\left(\sqrt{\frac{\gamma_{FSO}}{\gamma_{thFSO}}}\right) - \frac{\sigma_I^2}{2}}{\sigma_I}\right), \quad (18)$$

$$F(\gamma_{thRF}) = 1 - Q_1\left(\sqrt{2K}, \sqrt{2(K+1)\frac{\gamma_{thRF}}{\gamma_{th}}}\right), \quad (19)$$

where Q and Q_1 represent the Gaussian function and first order Marcum Q-function, respectively. Using (12) and (16), then (18) and (19) can be expressed as:

$$P_{out}(FSO) = Q\left(\frac{\ln\left(\frac{h_{l1}P_t}{P_{th1}}\right) - \frac{\sigma_I^2}{2}}{\sigma_I}\right), \quad (20)$$

$$P_{out}(RF) = 1 - Q_1\left(\sqrt{2K}, \sqrt{2(K+1)\frac{P_{th2}}{h_{l2}P_t}}\right), \quad (21)$$

P_{th1} and P_{th2} are threshold transmit powers (per bit) required to guarantee the target BERs for the FSO and RF subsystems. Their expression is given by [12]:

$$P_{th1} = \sqrt{\frac{\gamma_{thFSO}\ \sigma_{n1}^2}{R^2}} \quad (22)$$

$$P_{th2} = \frac{\gamma_{thRF}\ \sigma_{n2}^2}{\log_2(M)} \quad (23)$$

V. Application of Raptor Codes in Hybrid FSO/RF Systems

In this work, a practical soft-switching hybrid FSO/RF is designed and implemented using short-length Raptor codes (k=16). In fact, Raptor codes are an extension of Luby Transform (LT) codes. This extension consists to improve the resistance of LT codes by adding a pre-coder (e.g., LDPC codes). Raptor coding technique is developed as follows:

From initial k number of input packets, a sequence of an infinity Raptor encoded outputs packets are generated. The transmitter continues sending the encoded packets until 1-bit feedback is received from the receiver. The feedback is sent once the receiver decodes the entire message after that a sufficient number of not discarded packets are received.

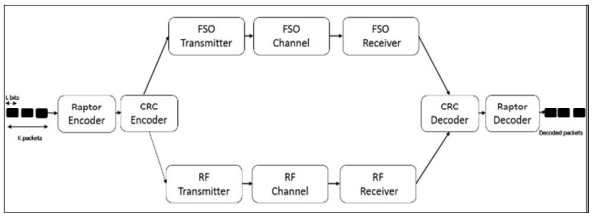

Fig. 3 Soft switching hybrid FSO/RF link using packet-level Raptor codes

Notice that in soft switching configuration there is no coordination between the FSO and RF links as illustrated in Fig. 3. The two links work independently and the packets are sent either on RF or FSO channels at their respective transmission rates.

A. LDPC Codes

LDPC codes are selected to be systematic. In fact, the systematic property provides the first k messages without coding after the pre-coding step as shown in Fig. 4. The pre-coding enlarges the effective number of message packets from k to k_1 where $(k - k_1)$ is the redundant packets each of degree D [13]. The LDPC codes are characterized by a sparse parity-check matrix H and a generator matrix G which are used in the encoding and decoding steps. The implementation of LDPC codes is performed according to the following steps given by [13].

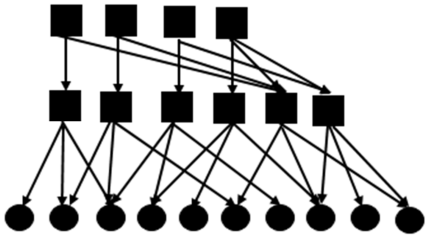

Fig. 4 Concept of Raptor codes design

B. LT Codes

Once the LDPC encoded packets, also called "intermediate symbols", are generated, the *LT* encoder starts to generate the output symbols. Each *LT* encoded packet has a degree $D_1(i)$ which is chosen randomly according to a distribution given by [13].

In [6], for $k = 16$ a heuristic technique is applied to find the distribution of degree termed Ω(x) with a good performance which is formulated as:

$$\Omega(x) = 0.18\,x + 0.52\,x^2 + 0.1\,x^3 + 0.2\,x^4.$$

where x^i is an *LT*-encoded packet of degree i.

VI. Implementation of Raptor Encoder and Decoder

The design of encoder and decoder algorithms is performed according to [6, pp. 5-6].

A. Raptor Encoder

In order, to simplify the decoding process, for each encoded Raptor packet of length *l* an index of $8 + log_2(k)$ bits must be added as shown in Fig. 5. This index referred to a set of table termed "connection information table" *CIT* which is stored at both transmitter and receiver side. This table contains all the "connection information *CI* of all encoded packets. In fact, the *CI* of an encoded packet contains the degree and all messages packets formed it. Thereafter, once the packet is encoded a CRC (Cyclic Redundancy Check) is applied and the encoded packet is send to the receiver.

CRC	Index	Data
(8 bits)	(12 bits)	(L bits)

Fig. 5 Encoded packet structure

B. Raptor Decoder

In the decoder process we defined three memory spaces: UP contains the un-decoded packets, NP contains the new release packet which released in the current decoding phase and DP contains the decoded packets which have been released in previous decoding stages. The modified BP algorithm can be summarized in five steps:

1) Check the CRC of the received packet. If the packet is incorrect then it will be crushed. Else, the index will be translated to the CI by lookup in the CIT.
2) If the received packet has a degree one, it will be stored in NP. Otherwise, it will be placed in UP. Then the received packet will be XOR-ed with any previously decoded packet in DP (of course the XOR operation is made in case where DP contains a decoded packet which presents one of the combined packets formed the received message). This step may reduce the degree of received packet or leads to the appearance of packet of degree one which will be saved in NP.
3) The packets in NP are used to repeat the step 2 until no packets of degree 1 are released.
4) All the NP packets will be copied to DP.
5) If all the initial k packets are recovered (decoded), the decoding process stops and one bit feedback will be sent to the transmitter in order to stop sending messages. Otherwise, wait the next received packet and repeat the step1.

C. Field Programmable Gate Array (FPGA)

The hybrid FSO/RF systems installed in QU campus has two Ethernet interfaces with a rates 1Gbit/s and 100 Mbps for FSO and RF links, respectively. Due to its advantages, we used the FPGA development kit NETFPGA-1G-CML in the implementation and design of soft switching configuration, (see Fig. 6). In fact, the FPGA has multiple Ethernet interfaces and can ensure a high capacity to support data rates of the two links [15]. Moreover, the NetFPGA-1G-CML board has 512 MB of 800 MHz DDR3 that can support high throughput packet buffering and uses low jitter 200 MHz oscillator that is required to speed up encoding/decoding algorithms. In this

work, we used two FPGAs which are installed in the transmitter and receiver side, respectively.

Fig. 6 NetFPGA-1G-CML

VII. Simulation and Results

Based on the modeling equations analysis and the assumed set of the operating parameters shown in Table I, we present the simulation results of the system behavior under different strength of turbulence related to Doha climate depicted in Table II.

TABLE I
FSO and RF Links Parameters

Symbol	Quantity	Value
λ	Laser wavelength	1550 nm
-	FSO modulation	OOK
R	Photodetector responsivity	0.5 A/W
D	Receiver diameter	20 cm
σ_{n1}^2	Noise variance	10^{-14} A^2
θ	Beam divergence angle	2 mrad
R_{FSO}	FSO data rate	1 Gb/s
-	RF modulation	16-QAM
F	Carrier frequency	60 GHz
B	Bandwidth	250MHz
G_t	Transmitter antenna gain	44 dBi
G_t	Receiver antenna gain	44 dBi
R_{RF}	RF data Rate	100 Mb/s

TABLE II
Weather Parameters

Weather Condition	Refractive index (C_N^2)	Attenuation (dB/km)
Heavy haze	9.5332×10^{-14}	7.8979
Moderate haze	9.6434×10^{-14}	1.4113
Heavy haze	$10..45 \times 10^{-14}$	0.445

Note that the parameters were calculated according to the climate parameters of Qatar using [8]-[14].

As shown in Figs. 7-9, increasing the strength of turbulence leads to increasing the outage probability of the FSO link which in turn decreases the performance of the total hybrid FSO/RF. In fact, where the strength of turbulence increases, the BER increases gradually until the FSO link becomes unavailable. Thus, in this case the transmitted data will be routed by the RF link which is more robust against atmospheric turbulence. System shows better link availability than each channel individually.

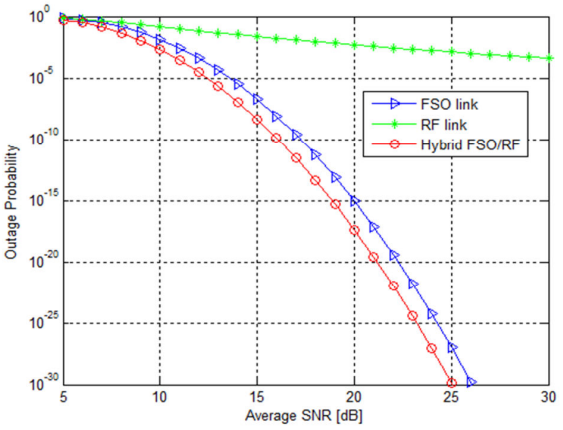

Fig. 7 Outage probability over atmospheric turbulence $\beta^2 = 0.3$

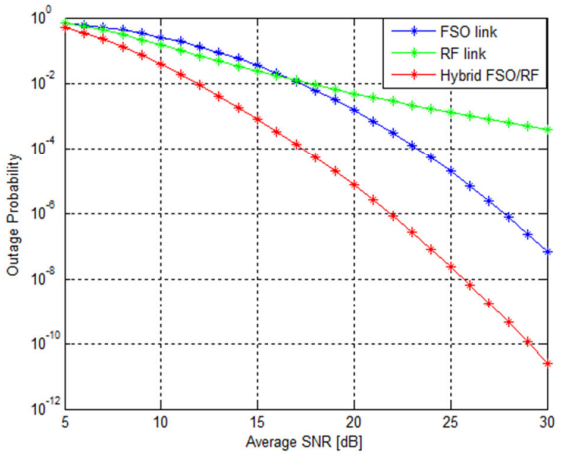

Fig. 8 Outage probability over atmospheric turbulence $\beta^2 = 0.5$

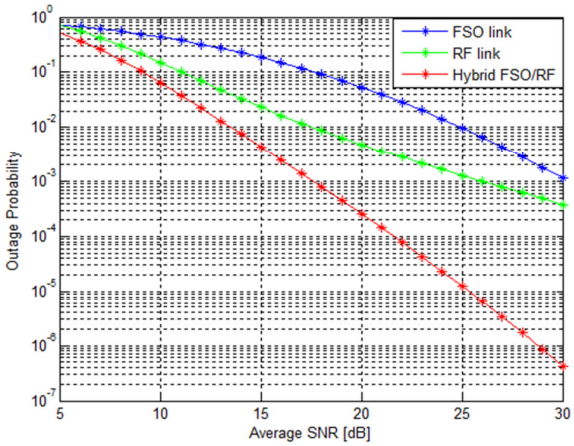

Fig. 9 Outage probability over atmospheric turbulence $\beta^2 = 0.8$

Using (20)-(23), we present the outage probability of FSO/RF links under hazy weather in Doha as a function of transmitted power Fig. 10. For all haze levels while the FSO is in outage, the hybrid follows the RF link, which maintains the data transmission. Once the FSO becomes available, the

system follows this link, and the outage probability of the hybrid becomes lower than that of each individual link. This is due to the availability of two links.

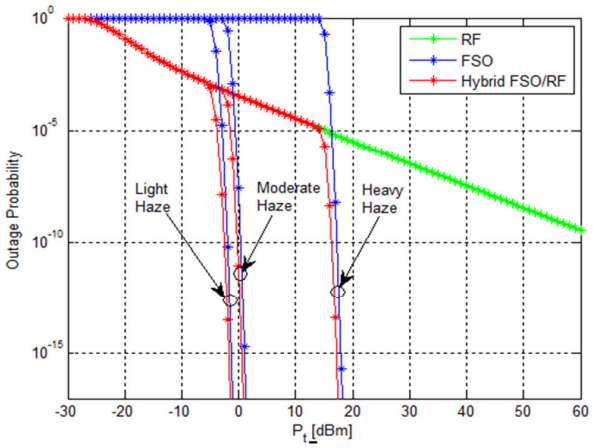

Fig. 10 Outage probability of hybrid FSO/RF systems under hazy weather

For a light haze the FSO link is in outage ($P_{out} = 1$) while $P_t = -6\,dBm$. Then the outage decreases gradually by increasing the transmit power. For a moderate or heavy haze, the FSO remains in outage for P_t less than almost -3 dBm and 14dBm, respectively. In fact, increasing the transmission power improves the signal quality and decreases the BER. For all haze levels, the hybrid performs better than any individual link. We noted that the thicker the haze becomes, the more the power required to operate the FSO and the hybrid FSO/RF increases. For light haze, $P_t = -6\,dBm$ and $P_t = -3\,dBm$ for moderate haze and 14 dBm for heavy haze.

As mentioned above, we implemented the raptor code to ensure the soft switching between the FSO and RF links.

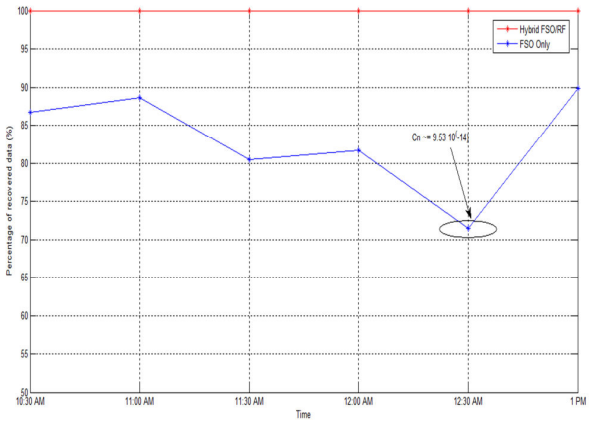

Fig. 11 Comparison of the percentage of received data of FSO link and Hybrid FSO/RF soft switching

As shown in Fig. 11, we presented the test results of June 13 from 10:30 AM to 01 PM. We notice that a big amount of data sent through the FSO link is lost at 12:30 pm. In fact, only 70% of data is recovered and the 30% data lost necessitates a retransmission. This loss can be accounted for by the high level of temperature and the big quantity of solar irradiance which can affect strongly the optical transmission. In contrary, in soft switching approach all the transmitted data are recovered (experimentally). In fact, using Raptor codes the loss of data is not an issue for data transmission. Thus, initially these codes are used as a solution for the data loss: If some packets are missing Raptor decoding is responsible of the recovery of the input symbols from the collected packets. Note that the outage probability of Raptor code depends only on "outage decoding" related to BP algorithm which is not our interest in this paper.

If we assume that the transmitted power of our system is 16 dBm. So, we can make a comparison between simulation and experimental results. From Fig. 10, we can identify the outage probability of FSO/RF systems. In fact, for light and moderate haze, the hybrid FSO/RF systems are available and can support the data transmission whereas for heavy haze the FSO link is in outage while $P_t < 16\,dBm$. In this case, the data will be routed by the RF link. The outage probability of the total hybrid is 10^{-8} while for FSO link is 10^{-3} (high level of BER).

Regarding the experimental tests, we found that for the same turbulence strength $C_n^2 = 9.53\ 10^{-14}$ a big amount of data sent through the FSO link are lost (30%). On other hand, in soft switching configuration all data are recovered. Thus, experimental and simulation results indicate that the soft switching approach enabled the hybrid FSO/RF to ensure better link availability than each link operating individually.

VIII. Conclusion

In this paper, we presented the different challenges that can weaken the optical signal. We focused on the refractive index in Qatar weather. We found that the atmospheric turbulence in Doha is quite high. We modulated the fading in FSO/RF channels by using a finite state Markov chain. Then we analyzed the outage probability of the hybrid FSO/RF under different strengths of turbulence related to Doha climate. Therefore, we designed and implemented a practical soft-switching hybrid FSO/RF using short-length Raptor. Simulation and experimental results showed that the hybrid FSO/RF ensures a reliable transmission and performs well than each individual link.

Acknowledgment

This publication was made possible by NPRP grant # 5-157-2-051 from the Qatar National Research Fund (a member of Qatar Foundation).

References

[1] H. G. Yong and al., "Free space optical communication using visible light", Journal of Zhejiang University Science.
[2] M. A. Ali, "Free space lasers propagation at different weather conditions"', Al Mustansiriyah, J. Sci, Vol. 23, No 2, 2012.
[3] M. Rouissat and al., "Free space optical channel characterization and modeling with focus on Algeria weather conditions", Journal of Computer Network and Information Security, 2012.
[4] I. E. Lee and al., "Practical implementation and performance study of a hard switched hybrid FSO/RF Link under controlled fog environment",

9th International Symposium on Communication Systems, Networks & Digital Sign (CSNDSP), 2014 .
[5] H. Tapse and al., "'Hybrid optical/RF channel performance analysis for Turbo codes"', *IEEE transactions on communications, Vol. 59, No. 5, 2011.*
[6] W. Zhang, S. Hranilovic, "Soft switching hybrid FSO/RF links using short-length Raptor codes: Design and implementation", *IEEE Journal on selected areas in communications, Vol. 27, No. 9, 2009.*
[7] M. Al Naboulsi and al, "Propagation of optical and infrared waves in the atmosphere", *pp. 481-495, 2005.*
[8] A. Alkholidi and K. Altowij, "effect of clear Atmospheric turbulence on quality of free space optical communications in western Asia", *ISBN: 978-953-51-0170-3, 2012.*
[9] A. Majumdar, "Free-space laser communication performance in the atmospheric channel", *Journal of optical Communication, 2005.*
[10] A. N. Zaki and al., "Dramatic atmospheric turbulence effects on submarine laser communication Systems and free space optics", *International Journal of Advanced Research in Computer Engineering & Technology (IJARCET), Vol. 3, March 2011.*
[11] H. Mouradi and al., "Reconfiguration modeling of reconfigurable hybrid FSO/RF links", *IEEE, ICC, 2010.*
[12] H. Kazemi, M. Uysal and F. Touati, "Outage analysis of hybrid FSO/RF systems based on finite state Markov chain modeling", *3rd international workshop in optical wireless Communications, 2014.*
[13] A. Shokrollahi, "Raptor codes", *June 19, 2003.*
[14] "http://www.timeanddate.com/weather/qatar/doha/historic", (*Online).*
[15] https://digilentinc.com/Data/Products/NETFPGA-1G-CML, (*Online), July 2014.*

Abir Touati Obtained her B.Sc., in Communications and Networks Engineering from National School of Engineering Gabes, Tunisia, in 2012. She received her M.SC from National School of Engineering (ENIT), Tunisia, in December 2013. She is a PhD. Student at SYSCOM, ENIT and currently she joining Qatar University as a Research Assistant.

Syed Jawad Hussain obtained his B.Sc. in Electrical Engineering from. International Islamic University Islamabad, Pakistan, in 2008. Currently he joining Qatar University as a Research Assistant.

Farid Touati obtained his B.Sc. in Electrical Engineering from the National School of Engineering Monastir, Tunisia, in 1988. He received his M.Sc. and Ph.D. from Nagoya Institute of Technology (NIT) of Japan in 1992 and 1995, respectively. He has joined Qatar University as an Associate Professor, in 2010. He has published more than 70 papers in several international journals and conferences. He has carried out successfully several grant projects in different countries in strategic areas like Bio-Engineering and Technology, Smart Irrigation, and Wireless Monitoring of Renewable Energy stations. Dr. Touati is a member of the Institute of Electrical and Electronics Engineers (IEEE), the American physical Society (APS), the International Association of Science and Technology (IASTED) of USA.

Ammar Bouallegue is a Professor in National School of Engineering (ENIT), Tunisia. He has published more than 90 papers in several international journals and conferences. Pr. Dr. Ammar is a member of the Institute of Electrical and Electronics Engineers (IEEE), and Swiss Federal Institute of Technology Zurich.